Inorganic Chemistry

Article

pubs.acs.org/IC

Synthesis, Crystal Structure, and Spectroscopy of the Mixed-Valent Boroseleniteselenate $B_2Se_3O_{10}$

Michael Daub,[†] Harald Scherer,[†] and Harald Hillebrecht*[,†,‡]

[†] Institut für Anorganische und Analytische Chemie, Albert-Ludwigs-Universität Freiburg, Albertstrasse 21, D-79104 Freiburg, Germany

[‡]Freiburger Materialforschungszentrum Stefan-Maier-Strasse 25, D-79104 Freiburg, Germany

Supporting Information

ABSTRACT: The first mixed-valent boroseleniteselenate $B_2Se_3O_{10}$ was obtained as a colorless, hygroscopic compound from the reaction of boric acid (H_3BO_3) in concentrated selenic acid (H_2SeO_4) at 265 °C. H_2SeO_4 can be replaced by appropriate amounts of SeO_2 and H_2O_2. The crystal structure was determined from single-crystal data ($P2_1/c$, Z = 4, a = 4.3466(2) Å, b = 7.0237(4) Å, c = 22.1460(9) Å, β = 94.922(2)°, R1 = 0.036, wR2 = 0.096). It represents a new structure type that is characterized by a 3D net of BO_4 tetrahedra, $Se^{VI}O_4$ tetrahedra, and trigonal-pyramidal $Se^{IV}O_3$ in a ratio of 2:1:2. ^{77}Se magic-angle-spinning NMR investigations confirm the mixed-valent character because the chemical shifts are found in the typical regions, i.e., 1278 and 1202 ppm for Se^{IV} and 972 ppm for Se^{VI}. The vibrational spectra show the typical modes according to the present polyhedra. In addition, NMR and vibrational spectra of the closely related $B_2Se_2O_7$ are presented.

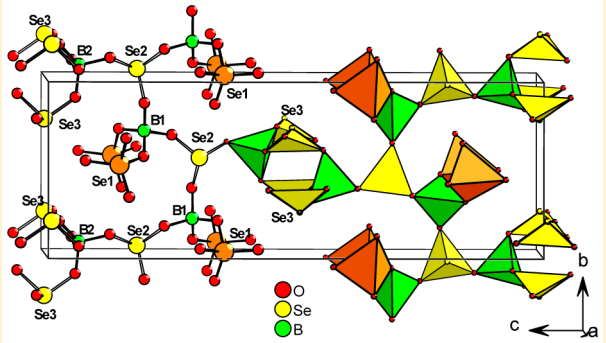

INTRODUCTION

Oxidic framework structures are the most important class of compounds for optical and other physical properties. The properties of interest may result from different reasons, for example, the corresponding cations itself (rare earth, transition metals, n_s^2 cations, etc.) or the symmetry of the crystal structure (ferroelectrics, piezoelectrics, nonlinear optical, etc.).

In the case of oxidic compounds of group 16 elements, it is well-known[1] that there is an interplay of the oxidation states IV + and VI+. The different states of oxidation can easily be seen from the building units. In oxidation state VI+, there are usually $[EO_4]^{2-}$ tetrahedra (E = S, Se, Te) or $[TeO_6]^{6-}$ octahedra, while in oxidation state IV+, trigonal nonplanar units $[EO_3]^{2-}$ are common, in agreement with the valence-shell electron-pair repulsion rules. This results in many structural similarities for the different representatives of E.

The chemistry of sulfur/oxygen species is dominated by compounds derived from SO_3/H_2SO_4, although there are many examples for deviations like sulfites or thiosulfates.[1] In the case of selenium, the situation is comparable but with different priorities.

Despite the close structural similarity between sulfur and selenium, their chemical properties show significant differences. For pH 0, the corresponding potentials are for SO_4^{2-}/SO_2 +0.158 V and for SeO_4^{2-}/SeO_2 +1.15 V.[1a] This might explain why selenates are much rarer in contrast to the oxides of sulfur. In the course of our systematic research for new oxidic framework structures, we have characterized the first borosulfates as alkali compounds.[2] In a continuation of this work, we successfully synthesized the analogous boroselenates by the exchange of sulfuric acid with selenic acid[3] and obtained and characterized the first diselenates $A_2Se_2O_7$.[4] Furthermore, we obtained a unique mixed-valent boroseleniteselenate $B_2Se_3O_{10}$ or $B_2(SeO_3)_2(SeO_4)$, and it is reported in this contribution.

The different behavior of SO_2/SO_4^{2-} and SeO_2/SeO_4^{2-} becomes also obvious in the current knowledge of ternary oxides B/S/O and B/Se/O, respectively. For each system, only one compound is known. While $B_2S_2O_9$ is a borosulfate with sulfur in oxidation state VI+,[5] the boroselenite $B_2Se_2O_7$ is a selenium(IV) compound.[6]

Mixed-valent selenium(IV)/selenium(VI) compounds are known. Besides the binary Se_3O_7,[7] there is the mineral Schmiederit $Pb_2Cu_2(OH)_4(SeO_3)(SeO_4)$[8] and a few more synthetic compounds like $Li_2Cu_3(SeO_3)_2(SeO_4)$,[9] $Er_2(SeO_3)_2(SeO_4)_2H_2O$,[10] $NaSm(SeO_3)(SeO_4)$,[11] $Hg_3(SeO_3)_2(SeO_4)$,[12] $Au_2(SeO_3)_2(SeO_4)$,[13] $Th(SeO_3)SeO_4)$,[14] $Bi_2(SeO_3)_2(SeO_4)$,[15] and $Sc_2(SeO_3)_2(SeO_4)$.[16] The special interest in selenites comes from the polar SeO_3 units, which support the occurrence of useful optical properties[17] and enhance nonlinear-optical properties[18] and polarizability.[19]

Received: December 10, 2014
Published: February 19, 2015

DOI: 10.1021/ic502916j
Inorg. Chem. 2015, 54, 2325−2330

EXPERIMENTAL SECTION

Synthesis. $B_2Se_3O_{10}$ can be synthesized from boric acid in selenic acid. A total of 121.3 mg (2 mmol) of $B(OH)_3$ and 1 g (6.6 mmol) of H_2SeO_4 were put into a silica glass crucible. The mixture was heated in air up to 265 °C at a rate of 3 °C/h. Then the oven was turned off, and the product formed as a colorless, crystalline, and very hygroscopic powder. The products were stored and handled in an argon-filled glovebox. The use of H_2SeO_4 can be substituted by an appropriate amount of SeO_2 and H_2O_2, which generates H_2SeO_4 "in situ". $B_2Se_2O_7$ was synthesized according to the literature[6] to draw a comparison (vibrational spectra and NMR data) to $B_2Se_3O_{10}$.

Characterization. *Powder X-ray Diffraction (XRD).* The products were characterized by powder XRD (STOE Stadi P, Mo Kα_1 radiation, Ge monochromator, image-plate detector, Debye–Scherrer geometry, transmission). Experimental and calculated diagrams of $B_2Se_3O_{10}$ and $B_2Se_2O_7$ show excellent agreement and a single-phase product. Data are given in Figures S1 and S2 in the Supporting Information (SI).

Vibrational Spectroscopy. Raman spectra were recorded by a Bruker FRA 106/S module with a Nd:YAG laser (λ = 1064 nm). IR spectra were recorded on a Nicolet Magna 760 spectrometer using a Diamond Orbit ATR unit (extended ATR correction with a refraction index of 1.5 was used).

Structure Solution and Refinement. Single crystals were prepared under an argon atmosphere. A data set for structure solution and refinement was recorded at 150 K using a Bruker AXS CCD APEX II diffractometer equipped with a microsource (Mo Kα radiation). Data reduction, unit cell refinement, and absorption correction were done with software of the supplier.[20,21] Structure solution and refinement were carried out without peculiarities (*SHELXL*[22] and Tables 1–3). Further details are available upon request at Fachinformationszentrum Karlsruhe, Hermann-von-Helmholtz-Platz 1, D-76344 Eggenstein-Leopoldshafen, Germany [fax (+49)724-808-666; e-mail crysdata@fiz-karlsruhe.de] with the depository number CSD 428810.

Table 1. Crystallographic Data and Details of the Refinement of $B_2Se_3O_{10}$

temperature [K]	150
color, size, shape	colorless, fragment
cryst syst	monoclinic
space group	$P2_1/c$
lattice parameters [Å]	
a [Å]	4.3466(2)
b [Å]	7.9237(4)
c [Å]	22.1460(9)
β [deg]	94.922(2)
Z	4
density (X-ray)[g/cm^3]	3.658
diffractometer	Bruker AXS CCD APEX II
radiation	Mo Kα, microsource
abs corrn	multiscan (*SADABS*[21])
$\mu_{\text{Mo K}\alpha}$ [mm^{-1}]	14.564
R_{int}/R_σ	0.0280/0.0279
range of indices	$-6 \le h \le 6$, $-11 \le k \le 9$, $-31 \le l \le 31$
$\theta_{\max}$ [deg]	30
measd/indep reflns	8107/2270
$N'(hkl)$ [$I > 2\sigma(I)$]	2037
no. of variables	139
GOF on F^2	1.280
R values [for reflections with $I \ge 2\sigma(I)$]	R1 = 0.0361, wR2 = 0.0915
R values (all data)	R1 = 0.0427, wR2 = 0.0965
residual electron density (max/min/σ) [e/Å^3]	2.47/−2.81/0.67

Table 2. Atomic Positions and Displacement Parameters U_{eq} [Å^2] of $B_2Se_3O_{10}$ with Standard Deviations in Parentheses

atom	x/a	y/b	z/c	U_{eq}
Se1	0.07829(14)	0.96721(8)	0.35667(3)	0.00614(15)
Se2	0.48327(14)	0.45600(8)	0.31277(3)	0.00532(15)
Se3	−0.20848(14)	0.72282(8)	0.50471(3)	0.00516(15)
O11	0.2341(12)	0.1400(6)	0.3400(2)	0.0142(10)
O12	−0.0277(12)	0.9487(7)	0.4239(2)	0.0142(15)
O13	0.3237(10)	0.8039(6)	0.3473(2)	0.0077(8)
O14	−0.2228(11)	0.9350(6)	0.3038(2)	0.0076(8)
O21	0.6417(11)	0.3366(6)	0.2597(2)	0.0076(8)
O22	0.7226(10)	0.3797(6)	0.3710(2)	0.0062(8)
O23	0.6860(11)	0.6383(6)	0.3007(2)	0.0086(8)
O31	0.1748(10)	0.7004(6)	0.5253(2)	0.0066(8)
O32	−0.2350(11)	0.6011(6)	0.4413(2)	0.0074(8)
O33	−0.3385(11)	0.5869(6)	0.5572(2)	0.0083(9)
B1	0.5383(16)	0.8028(9)	0.2991(3)	0.0053(11)
B2	−0.3315(16)	0.4240(9)	0.4331(3)	0.0067(12)

NMR Spectra. The solid-state ^{77}Se magic-angle-spinning (MAS) NMR spectra were measured on a Bruker DSX 500 spectrometer equipped with a 4 mm MAS probe, operated at rotational frequencies of 5–12 kHz. There were 2000–5000 transients accumulated using one-pulse experiments with pulses of 3 μs length and relaxation delays of 45 s. Experiments carried out with different relaxation times resulted in comparable intensity ratios of the signals observed. Adamantane was used as an external reference. On the basis of the measured intensities, distribution of the MAS rotation sidebands was found. Spectra with different frequencies are shown in Figure S3 in the SI. The solid-state ^{11}B MAS NMR spectra were detected using a one-pulse experiment with pulses of 1 μs length and relaxation delays of 60 s accumulating 4096 scans. Chemical shifts are given with respect to Me_2Se for ^{77}Se and BF_3*Et_2O for ^{11}B. For measurement and processing of the data, the software *Topspin 2.1* and *Topspin 3.2* from Bruker were used.

RESULTS AND DISCUSSION

Crystal Structure. The crystal structure of $B_2Se_3O_{10}$ represents a new structure type, and the first mixed-valent boroseleniteselenate with selenium(VI) and selenium(IV) in a ratio of 1:2 was obtained. The structure is characterized by a 3D framework of the well-known moieties of boroselenates and boroselenites, i.e., BO_4 tetrahedra with SeO_4 tetrahedra and trigonal-pyramidal SeO_3 units (Ψ tetrahedra), respectively. Figure 1 shows this framework of corner-sharing polyhedra. All atoms are located on general positions. The number of symmetry different atoms reflects directly the function within the framework, where selenium polyhedra are connected exclusively to BO_4 tetrahedra and vice versa. The tetrahedron of B2 is only linked to $Se^{VI}O_3$ units, three with Se1 and one with Se2 (Figure 2a). The tetrahedron of B1 belongs to two SeO_4 tetrahedra (Se3) and two SeO_3 (Se2) units (Figure 2b). The 3D framework of polyhedra can be divided into chains of alternating BO_4 and SeO_4 tetrahedra running in the direction of the short a axis and chains of dimeric units formed by the polyhedra around B2 and Se1. These two elements are connected by the SeO_3 units with Se2. The 3-fold axis of the SeO_3 units are parallel to the b axis (Se1) and a axis (Se2). The orientation of the lone pairs follows the 3-fold axes and shows two different patterns. In the case of Se1, they are arranged like a zipper, forming channels in the direction of the a axis (x, $^1/_2$, 0 and x, 0, $^1/_2$). For Se2, the Ψ tetrahedra form polar chains with antiparallel orientation (polar direction [100] and [−100]), respectively.

DOI: 10.1021/ic502916j
Inorg. Chem. 2015, 54, 2325–2330

Table 3. Selected Distances (Å) and Angles (deg) for $B_2Se_3O_{10}$

B1–O23	1.452(8)	B2–O22	1.459(8)	O–B1–O	104.5(5)–115.5(5)
B1–O14	1.472(8)	B2–O33	1.471(8)	O–B2–O	105.9(5)–117.7(5)
B1–O13	1.477(8)	B2–O32	1.471(8)		
B1–O21	1.483(8)	B2–O31	1.475(8)		
Se1–O11	1.585(5)	Se3–O31	1.699(4)	O–Se1–O	104.8(2)–117.3(3)
Se1–O12	1.602(5)	Se3–O32	1.699(4)	O–Se2–O	94.0(2)–97.3(2)
Se1–O14	1.699(5)	Se3–O33	1.715(5)	O–Se3–O	97.2(2)–101.6(2)
Se1–O13	1.701(5)				
Se2–O22	1.697(4)				
Se1–O21	1.701(4)				
Se1–O23	1.725(5)				

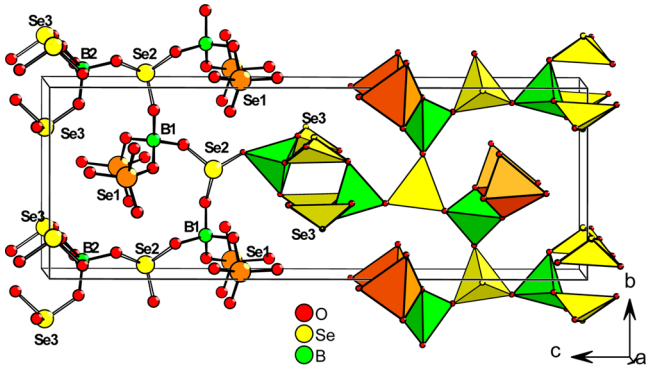

Figure 1. Crystal structure of $B_2Se_3O_{10}$.

The distances and bonding angles (Table 3) are as expected and fit to the values known from other boroselenites ($B_2Se_2O_7$)[6] and boroselenates.[3] The BO_4 tetrahedra are quite regular, with distances between 1.452(8) and 1.477(8) Å and angles between 104.5(5)° and 116.7(5)°. The SeO_3 units are very regular and similar. Distances are between 1.697(4) and 1.725(5) Å and O–Se–O angles between 94.0(2)° and 101.6(2)°. Different Se–O distances occur in the SeO_4 tetrahedron according to the different topological properties. The terminal Se–O bonds are significantly shorter [1.585(5)/1.602(5) Å] than the bridging ones [1.699(5)/1.701(5) Å]. This leads to a distortion of the tetrahedron [O^{term}–Se–O^{term}, 117.3(2)°; O^{br}–Se–O^{br}, 104.8(2)°]. Furthermore, the displacement parameters of terminal oxygen atoms are slightly enlarged (Figure 2 and Table 2). The separation of the Se–O distances is expected and is similar to that of diselenates $A_2Se_2O_7$ (Se–O^{term}, 1.598–1.628 Å; Se–O^{br}, 1.750–1.807 Å).[4] Bond valence sums can be calculated according to the method of Brown.[23] They give a good measure of the plausibility of crystal structures and should allow one to distinguish between different oxidation numbers in mixed-valent compounds. The values for B1 and B2 are 3.13 and 3.15, respectively. The values for selenite atoms Se1 and Se2 are very similar also (3.96 and 3.90, respectively). The sum of Se3 as a selenate is 6.19. For the oxygen atoms, the values of the bridging ones are between 2.06 and 2.14, while those for the terminal ones are significantly lower (O31, 1.81; O32, 1.73). All in all, the bond valence sums are in good agreement with the expectations for mixed-valent boroseleniteselenate $B_2Se_3O_{10}$. Furthermore, bond valence sums of comparable compounds should yield similar values if the crystal structure is properly described.

A check of the plausibility of the structure can also be done by a lattice energy calculation.[24] For $B_2Se_3O_{10}$, the lattice energy deviates less than 1% from the stoichiometric sum of the binary oxides B_2O_3,[25] SeO_2,[26] and SeO_3.[27] Electrostatic potentials for all atoms are listed in Table S1 in the SI.

The structure of $B_2Se_3O_{10}$ can be compared to the boroselenite $B_2Se_2O_7$.[6] Here, alternating BO_4 tetrahedra and trigonal-pyramidal SeO_3 are linked by common corners to layers perpendicular to [100]. The fourth oxygen atom of the BO_4 tetrahedron connects to the BO_4 tetrahedron of the subsequent layers (direction [100]). The bond valence sums of boron (3.10/3.12) and selenium (3.89/3.94) are similar to that of $B_2Se_3O_{10}$. Formally, the connectivity of $B_2Se_2O_7$ and

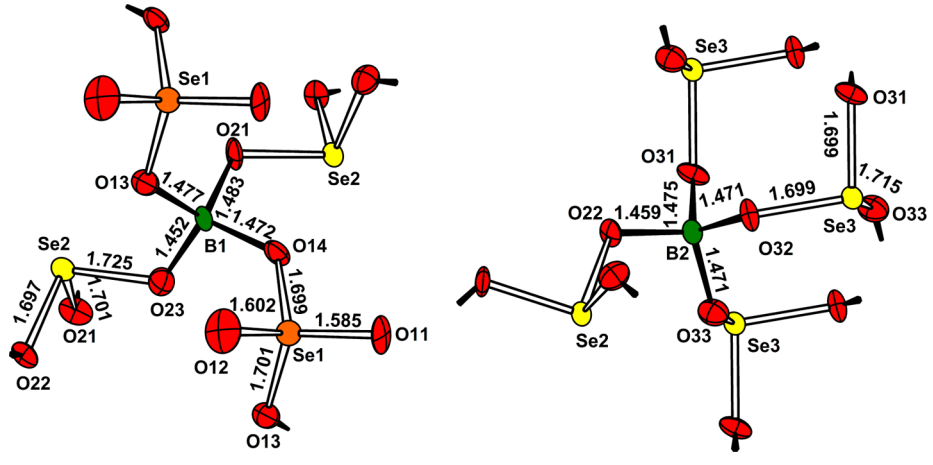

Figure 2. Surroundings of BO_4 tetrahedra in $B_2Se_3O_{10}$. Ellipsoids represent 90% probability.

DOI: 10.1021/ic502916j
Inorg. Chem. 2015, 54, 2325–2330

$B_2Se_3O_{10}$ can be related by substitution of the bridging O^{2-} anion between the two BO_4 tetrahedra in $B_2Se_2O_7$ by SeO_4^{2-}.

The structure of the mixed-valent Se_3O_7 was determined as a nitromethane adduct. The cyclic unit Se_3O_7 contains the same selenium polyhedra as $B_2Se_3O_{10}$, but the bond valence sums show larger deviations (Se^{VI}, 6.52; Se^{IV}, 3.66, 2.96), which might result from an inaccurate structure determination.

Other mixed-valent seleniteselenates $A_2Se_3O_{10}$ of trivalent elements A are $Bi_2Se_3O_{10}$,[15] $Sc_2Se_3O_{10}$,[16] and $Au_2Se_3O_{10}$.[13] In the bismuth compound, distorted BiO_6 octahedra connect layers of corner-linked SeO_4 tetrahedra and trigonal-pyramidal SeO_3 units to a 3D structure. Bond valence sum calculations for Se^{IV} and Se^{VI} result in values of 3.98−4.03 and 6.25, respectively. In $Sc_2Se_3O_{10}$, the scandium atoms are 7-fold-coordinated as pentagonal bipyramids. The bond valence sums are 4.06−4.10 (Se^{IV}) and 6.06 (Se^{VI}). In $Au_2Se_3O_{10}$, square-planar AuO_4 units, which are typical for gold(III) compounds, and SeO_3 units form layers that are connected by two oxygen atoms of the SeO_4 tetrahedra. Here, the bond valence sums are significantly lower than those for the other compounds (Se^{IV}, 3.67; Se^{VI}, 5.63).

The conditions for the formation of $B_2Se_3O_{10}$ fit to the general tendencies for the stability of the oxidation states of selenium. While the ternary boroselenite $B_2Se_2O_7$ is easily formed at elevated temperatures (320 °C, SeO_2 + B_2O_3) by direct combination of the binary oxides, $B_2Se_3O_{10}$ is formed by partial decomposition of the selenium(VI) compound H_2SeO_4 at room temperature. In comparison to the analogous sulfur compounds, the chemical and thermal stability of SeO_3/H_2SeO_4 is significantly lowered.

Vibrational Spectra. Figure 3 shows Raman and IR spectra of $B_2Se_3O_{10}$. For reasons of comparison, the spectra of $B_2Se_3O_7$

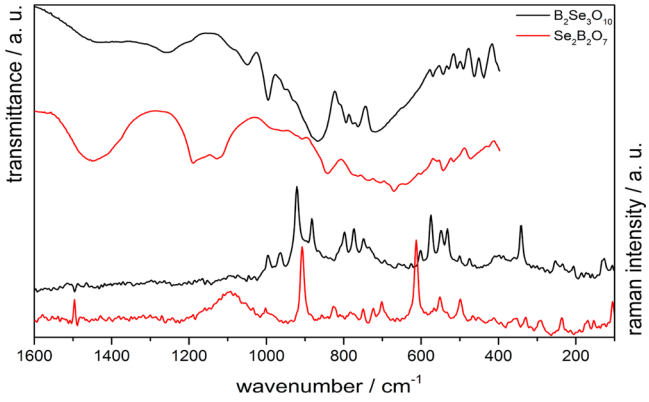

Figure 3. Vibrational spectra of $Be_2Se_3O_{10}$ (upper lines) and $B_2Se_2O_7$ (lower lines).

were additionally recorded and added to Figure 3. Obviously, the spectrum for $Be_2Se_2O_7$ is less complex than that for $Be_2Se_3O_{10}$ because of the additional SeO_4 tetrahedron instead of a bridging oxygen atom between the BO_4 tetrahedra. In a simplified view, the additional modes can be attributed to this difference. The tentative assignments of the modes in $Be_2Se_2O_7$ and $Be_2Se_3O_{10}$ are listed in Table 4.

For $B_2Se_2O_7$, the highest frequencies of the IR spectrum (1550−1350 cm^{-1}) can be attributed to the valence modes within the B_2O_7 unit and the lower frequencies (1230−1070 cm^{-1}) to the $Se^{IV}O_3$ units. The symmetric valence mode $\nu_s(SeO_3)$ (Raman, 908 cm^{-1}) is known from other selenites.[28]

Table 4. Observed Frequencies of the Vibrational Spectra with Feasible Assignments

$B_2Se_3O_{10}$		$B_2Se_2O_7$		
IR	Raman	IR	Raman	assignment
~1445		~1445	1496	
~1257		~1192		$\nu(BO_4)$
		~1130	1093	
997	997			$\nu(Se^{VI}O_2)$
	964			
	921		908	$\nu_s(Se^{IV}O_3)$
	883			
796	798	845		$\nu_{as}(Se^{IV}O_3)$
779	773			
766	750			
~717				ν_{as}(SeOSe)
			613	ν_s(SeOSe) + ν_s(BOSe)
	600−530			ν_s(SeOSe)

The asymmetric mode $\nu_{as}(SeO_3)$ (IR, 845 cm^{-1}) is found at lower values.

The B−O valence modes in $B_2Se_3O_{10}$ are between 1500 and 1200 cm^{-1} (IR). The modes of the O^{term}−Se bond of the SeO_4 tetrahedra are between 997 cm^{-1} (IR) and 964 cm^{-1} (Raman). The modes of the $Se^{IV}O_3$ units show up again at lower wavenumbers (Raman, ν_s 921−883 cm^{-1}; IR, ν_{as} 800−750 cm^{-1}). Below the region of the valence mode, we expect the deformation modes ν_{as}(SeOB) (IR: 717 cm^{-1}) and ν_s(SeOB) (Raman: 600−530 cm^{-1}).

The assignment of the modes between 1000 and 900 cm^{-1} to the SeO_4 tetrahedra is supported by the vibrational spectra of diselenates $A_2Se_2O_7$,[2d] where terminal Se−O modes are observed between 1000 and 950 cm^{-1}. The bridging modes are at lower frequencies. This is the range wherein the $B_2Se_3O_{10}$ modes of the $Se^{IV}O_3$ units appear, so a separation is not possible.

Vibrational spectra were also recorded for other mixed-valent seleniteselenates like $Au_2(SeO_3)_2(SeO_4)$,[13] $Bi_2(SeO_3)_2(SeO_4)$,[15] and $Sc_2(SeO_3)_2(SeO_4)$.[16] The general findings (modes up to 1000 cm^{-1}, higher frequencies for SeO_4 than for SeO_3, splitting by reduced site symmetry, etc.) are comparable to those for $B_2Se_3O_{10}$. Differences result obviously from the polyhedra of the additional building units, i.e., BO_4 tetrahedra in $B_2Se_3O_{10}$ and square-planar AuO_4 units in $Au_2(SeO_3)_2(SeO_4)$.

NMR Spectra. Figure 4 shows the ^{77}Se MAS NMR spectrum of $B_2Se_3O_{10}$. Additionally, spectra of $B_2Se_2O_7$ were measured as comparative data. Spectra obtained at further rotational frequencies are shown in Figures S3 and S4 in the SI. The limited signal-to-noise ratio prevented a reliable integration of the peaks, so the anisotropy parameters were not fitted. For $B_2Se_3O_{10}$, three sideband patterns centered at 972, 1202, and 1278 ppm can be seen. The signal at 972 ppm can clearly be assigned to Se^{VI}, while the other two belong to Se^{IV}. The Se^{IV} signals show a significant asymmetry that results from the trigonal-pyramidal coordination. $B_2Se_2O_7$ featured two side-band patterns centered at 1246 and 1278 ppm. Both are easily assigned to the two different Se^{IV} species. The values for $B_2Se_3O_{10}$ are in excellent agreement with $B_2Se_2O_7$ and other ^{77}Se NMR investigations.[29]

Figure 5 shows the ^{11}B NMR sepctra of $B_2Se_3O_{10}$. There is one signal at 1 ppm, which is typical for BO_4 tetrahedra. The two symmetry-independent boron atoms are not separated.

DOI: 10.1021/ic502916j
Inorg. Chem. 2015, 54, 2325−2330

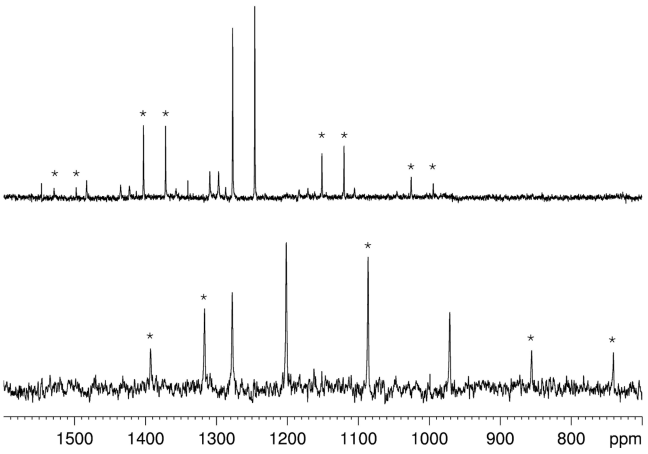

Figure 4. ^{77}Se MAS NMR spectra (95.4 MHz) of $Be_2Se_3O_{10}$ (top, 1996 scans, 11 kHz) and $B_2Se_2O_7$ (bottom, 4096 scans, 12 kHz) at room temperature. Rotational sidebands are marked with asterisks; weak additional signals in $B_2Se_2O_7$ result from decomposition products.

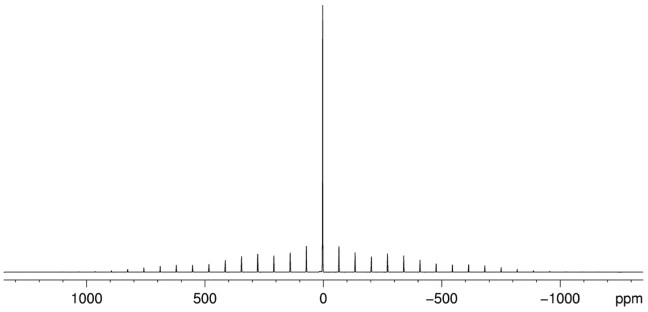

Figure 5. ^{11}B MAS NMR spectrum (160.5 MHz) of $B_2Se_3O_{10}$ at room temperature (4096 scans, 11 kHz).

The extent of rotational sidebands and the NMR spectra of $B_2Se_2O_7$ are shown in Figure S5 in the SI.

The best representative for comparison is $Au_2(SeO_3)_2(SeO_4)$. Wickleder et al. give signals at +87.9 and −235.5 ppm in a ratio of 2:1.[13] These values are very different because H_2SeO_3 served as a point of reference. Using the same point of reference, values of 1370 ppm (Se^{IV}) and 1046 ppm (Se^{VI}) are obtained.[29] So, our findings for $Be_2Se_3O_{10}$ and $B_2Se_2O_7$ are in good agreement. Both results follow the general tendency that higher coordination leads to lower resonance frequencies.[28] Recently, Haas and Jansen found 876 ppm for the trigonal-bipyramidal SeO_5 in Li_4SeO_5[30] and 667 ppm for the SeO_6 octahedra in $Na_{12}(SeO_6)(SeO_4)_3$.[31]

CONCLUSIONS

Mixed-valent seleniteselenates are a very small class of compounds. The mixed-valent character of the boroselenite-selenate $B_2Se_3O_{10}$ is easily seen in the structural features. SeO_4 tetrahedra and trigonal-pyramidal SeO_3 as typical building units are connected with additional BO_4 tetrahedra to a 3D network. The vibrational spectra of $B_2Se_3O_{10}$ can be assigned by comparison to diselenates $A_2Se_2O_7$ and the boroselenite $B_2Se_2O_7$. ^{77}Se and ^{11}B NMR spectra of $B_2Se_3O_{10}$ and $B_2Se_2O_7$ confirm the structural findings. In $B_2Se_3O_{10}$, the signals of Se^{IV} and Se^{VI} are clearly distinguishable. The two different Se^{IV} units are separated in both cases. The ^{11}B signals of the BO_4 tetrahedra are very similar.

The combination of tetrahedral units BO_4 and SeO_4 with trigonal-pyramidal SeO_3 leads to unique 3D framework structures, which might be interesting for optical applications. ^{77}Se and ^{11}B NMR spectra allow characterization of the building units without determination of the crystal structure. Even the evaluation of the vibrational spectra gives good information for the existing building units.

Besides the general interest in new optical materials, selenites and selenates were intensely investigated as materials with high proton conductivity. Boroseleniteselenates may represent a new polyhedra framework for superionic conductors. In this respect, it is important that we already have characterized boroselenates of alkali metals containing additional protons ($K_4H[B(SeO_4)_4]$) and oxonium cations $[(H_3O)Na_6[B(SeO_4)_4](SeO_4)$.[3] For the borosulfates, we found, besides an oxonium compound ($H_3O[B(SO_4)_2]$), even a polyacid ($H[B(S_2O_7)(SO_4)]$).[2c]

ASSOCIATED CONTENT

Supporting Information

X-ray crystallographic data in CIF format, experimental and calculated powder XRD patterns ($B_2Se_3O_{10}$ and $B_2Se_2O_7$), ^{77}Se and ^{11}B MAS NMR spectra at different rotational frequencies ($B_2Se_3O_{10}$ and $B_2Se_2O_7$), and electrostatic potentials ($B_2Se_3O_{10}$). This material is available free of charge via the Internet at http://pubs.acs.org.

AUTHOR INFORMATION

Corresponding Author

*E-mail: harald.hillebrecht@ac.uni-freiburg.de. Phone: 0049-761-203 6131. Fax: 0049-761-203 6102.

Notes

The authors declare no competing financial interest.

DEDICATION

Dedicated to Prof. Dr. Heinrich Vahrenkamp on the occasion of his 75th birthday.

REFERENCES

(1) (a) Holleman, A. F.; Wiberg, N. *Lehrbuch der Anorganischen Chemie*; Verlag de Gruyter: Berlin, 2007. (b) Housecroft, C. E.; Sharpe, A. G. *Inorganic Chemistry*; Prentice-Hall: Upper Saddle River, NJ2012.

(2) (a) Höppe, H. A.; Kazmierczak, K.; Daub, M.; Förg, K.; Fuchs, F.; Hillebrecht, H. *Angew. Chem.* **2012**, *124*, 6359−6362; *Angew. Chem., Int. Ed.* **2012**, *51*, 6255−6257. (b) Daub, M.; Kazmierczak, K.; Gross, P.; Höppe, H.; Hillebrecht, H. *Inorg. Chem.* **2013**, *52*, 6011−6020. (c) Daub, M.; Kazmierczak, K.; Höppe, H.; Hillebrecht, H. *Chem.—Eur. J.* **2013**, *19*, 16954−16962. (d) Daub, M.; Hillebrecht, H. *Z. Kristallogr., Suppl.* **2014**, *34*, 129. (e) Daub, M.; Höppe, H.; Hillebrecht, H. *Z. Anorg. Allg. Chem.* **2014**, *640*, 2914−2921.

(3) Daub, M.; Hillebrecht, H. *Chem.—Eur. J.* **2015**, *21*, 298−304.

(4) Daub, M.; Hillebrecht, H. *Z. Kristallogr., Suppl.* **2014**, *34*, 129.

(5) Logemann, C.; Wickleder, M. S. *Angew. Chem.* **2013**, *125*, 14479−14482; *Angew. Chem., Int. Ed.* **2013**, *52*, 14229−14232.

(6) Kong, F.; Huang, S.-P.; Sun, Z.-M.; Mao, J.-G.; Cheng, W.-D. *J. Am. Chem. Soc.* **2006**, *128*, 7750−7751.

(7) Touzin, J.; Kilian, P.; Zak, Z. *Z. Anorg. Allg. Chem.* **1996**, *622*, 1617−1622.

(8) Effenberger, H. *J. Solid State Chem.* **1987**, *70*, 303−312.

(9) Geister, G. *Monatsh. Chem.* **1989**, *120*, 661−666.

(10) Morris, R. E.; Wilkinson, A. P.; Cheetham, A. K. *Inorg. Chem.* **1992**, *31*, 4774−4777.

DOI: 10.1021/ic502916j
Inorg. Chem. 2015, 54, 2325−2330

(11) Krügermann, I.; Wickleder, M. *Z. Anorg. Allg. Chem.* **2002**, *628*, 147−151.
(12) Weil, M.; Kolitsch, U. *Acta Crystallogr., Sect. C* **2002**, *58*, i47−i49.
(13) Wickleder, M. S.; Büchner, O.; Wickleder, C.; el Sheik, S.; Brunklaus, G.; Eckert, H. *Inorg. Chem.* **2004**, *43*, 5860−5864.
(14) Sullens, T. A.; Almond, P. M.; Byrd, J. A.; Beitz, J. U.; Bray, T. H.; Albrecht-Schmitt, T. E. *J. Solid State Chem.* **2006**, *179*, 1192−1201.
(15) Lee, E. P.; Song, S. Y.; Lee, D. W.; Ok, K. M. *Inorg. Chem.* **2013**, *52*, 4097−4103.
(16) Song, S. Y.; Lee, D. W.; Ok, K. M. *Inorg. Chem.* **2014**, *53*, 7040−7047.
(17) (a) Zhang, J.-H.; Kong, F.; Yang, B.-P.; Mao, J.-G *CrystEngComm* **2012**, *14*, 8727−8733. (b) Rao, C. N. R.; Behera, J. N.; Dan, M. *Chem. Soc. Rev.* **2006**, *35*, 375−387. (c) Choudhury, A.; Kumar, U.; Rao, C. N. R. *Angew. Chem., Int. Ed.* **2002**, *41*, 158−161. (d) Harrison, W. T. A.; Phillips, M. L. F.; Stanchfield, J.; Nenoff, T. N. *Angew. Chem., Int. Ed.* **2000**, *39*, 3808−3810.
(18) Halasyamani, P. S.; Poeppelmeier, K. R. *Chem. Mater.* **1998**, *10*, 2753−2769.
(19) Ok, K. M.; Halasyamani, P. S. *Chem. Mater.* **2002**, *14*, 2360−2364.
(20) Remove, T. *SAINT, Data reduction and frame integration program for the CCD area-detector system*, ;Bruker Analytical X-ray Systems: Madison, WI, 2006.
(21) Sheldrick, G. M. *SADABS, Program for area detector adsorption correction*; Institute for Inorganic Chemistry, University of Göttingen: Göttingen, Germany, 1996.
(22) Sheldrick, G. M. *SHELXTL, V 5.10 Crystallographic System*; Bruker AXS Analytical X-ray Instruments Inc.: Madison, WI, 1997.
(23) (a) Brown, I. D. *J. Appl. Crystallogr.* **1996**, *29*, 479−480. (b) Adams, S. *softB*, version 0.96; 2004.
(24) (a) Hoppe, R. *Angew. Chem., Int. Ed. Engl.* **1966**, *5*, 95−106. (c) Hoppe, R. *Angew. Chem., Int. Ed. Engl.* **1970**, *9*, 25−34. (b) Hübenthal, R. *MAPLE, Program for the Calculation of the Madelung Part of Lattice Energy*; University of Gießen: Gießen, Germany, 1993.
(25) Gurr, G. E.; Montgomery, P.; Knutson, C. D.; Gorres, B. T. *Acta Crystallogr., Sect. B* **1970**, *26*, 906−915.
(26) Strahl, K.; Legros, J. P.; Galy, J. *Z. Kristallogr.* **1992**, *202*, 99−107.
(27) Pascard, R.; Pascard-Billy, C. *Acta Crystallogr.* **1965**, *8*, 830−834.
(28) Demko, B. A.; Wasylishen, R. E. *Prog. Nucl. Magn. Res.* **2009**, *54*, 208−238.
(29) Haas, A.; Jansen, M. *Z. Anorg. Allg. Chem.* **2000**, *626*, 1174−1178.
(30) Haas, A.; Jansen, M. *Z. Anorg. Allg. Chem.* **2001**, *627*, 1313−1318.
(31) (a) Troyanov, S. J.; Morozov, I. V.; Zakharov, M. A.; Kemnitz, E. *Crystallogr. Rep.* **1999**, *44*, 560−564. (b) Zakharov, M. A.; Troyanov, S. I.; Kemnitz, E. *Z. Kristallogr.* **2001**, *216*, 172−175.

DOI: 10.1021/ic502916j
Inorg. Chem. 2015, 54, 2325−2330